International Journal of Mathematical Archive-10(5), 2019, 49-61
Available online through www.ijma.info ISSN 2229 – 5046

# EFFECT OF NON-LINEAR RADIATION ON TRANSIENT CONVECTIVE HEAT TRANSFER FLOW OF A VISCOUS FLUID PAST A STRETCHING SURFACE WITH HALL EFFECTS, IN THE PRESENCE OF NON-UNIFORM HEAT SOURCE WITH CONSTANT HEAT FLUX AND PARTIAL SLIP

**CH SURESH*[1] AND DR. P.M.V. PRASAD[2]**

**[1]Research Scholar, Department of Mathematics,
Rayalaseema University, Kurnool, (A.P.), India.**

**[2]Associate Professor of Mathematics,
S. V. G. S. Degree College of Arts and Science, Nellore, (A.P.), India.**

***(Received On: 14-04-19; & Accepted On: 14-05-19)***

***ABSTRACT***

***I****n this chapter, we study the combined influence of Hall effects and radiation absorption on unsteady convective heat transfer flow of a viscous electrically conducting fluid through a porous medium past a stretching sheet in the presence of non-uniform heat source. The equations governing the flow of heat transfer have been solved by Galerkin Finite Element Analysis with three nodded line segments. The velocity, temperature have been analysed for different values of G,M, m, N, γ, A1, B1, Sc, Ec and $Q_1$. The rate of heat transfer on the plate has been evaluated numerically for different variations.*

***Keywords:*** *Radiation, Heat Transfer, Stretching Surface, Hall Effect, Heat Source.*

## 1. INTRODUCTION

Mixed convection boundary layer flow of a binary mixture of fluids with heat transfer past a continuous moving surface has attracted considerable attention in the past several decades, due to its many important engineering and industrial applications (22, 34). In nature such flows are encountered in the oceans, lakes, solar ponds, and the atmosphere. They are also responsible for the geophysics of planets. In industry, a familiar example of a binary mixture of fluids is an emulsion, which is the dispersion of one fluid within another fluid. Typical emulsions are oil dispersed within water or water within oil. Another example where the mixture of fluids plays an important role is in multigrade oils. Polymeric-type fluids are added to the base oil so as to enhance the lubrication properties of mineral oil. Moreover, the mixed convection boundary layer problem is also encountered in aerodynamic extrusion of plastic and rubber sheets, cooling of an infinite metallic plate in a cooling path, which may be an electrolyte, crystal growing, the boundary layer along a liquid film in condensation processes, and a polymer sheet or filament extruded continuously from a die or along thread traveling between a feed roll and a windup roll are examples of practical applications of continuous moving surfaces.

Several studies on boundary layer flow coupled with heat transfer have already appeared in the literature (11, 12, 27, 28, 30). Similarly, the Soret or thermo-diffusion effect is the contribution to the mass fluxes due to temperature gradients. Moreover, when chemical species are introduced at a surface in the fluid domain with different (lower) density than the surrounding fluid, both Soret (thermo-diffusion) and Dufour (diffusion-thermal) effects can be influential. The effect of diffusion-thermal and thermal diffusion of heat has been developed from the kinetic theory of gases by Chapman and Cowling (13) and Hirshfelder *et al.* (21) they explained the phenomena and derived the necessary formulas to calculate the thermal diffusion coefficient and the thermal-diffusion factor for monatomic gases or for polyatomic gas mixtures. Kafoussias and Williams (25) studied the thermal diffusion and the diffusion-thermal effects on mixed free-forced convective steady laminar boundary layer flow, over a vertical flat plate, with temperature dependent viscosity. Alam and Rahman (4) studied the Dufour and Soret effects on mixed convection flow past a vertical porous flat plate with variable suction. Anghel *et al.* (7) investigated the Dufour and Soret effects on free convection boundary layer over a vertical surface embedded in a porous medium. Postelnicu (31) studied the influence of a magnetic field on heat transfer by natural convection from a vertical surface embedded in an electrically

***Corresponding Author: Ch Suresh*[1]***
***[1]Research Scholar, Department of Mathematics, Rayalaseema University, Kurnool, (A.P.), India.***

conducting fluid-saturated porous medium considering Soret and Dufour effects with constant surface temperature and concentration. Alam *et al.* (6) presented an analysis of the Soret and Dufour effects on free convective heat transfer flow in a porous medium with time-dependent temperature and concentration. Beg *et al.* (9) investigated numerically the free convection magnetohydrodynamic heat transfer from a stretching surface to a saturated porous medium with Soret and Dufour effects. Various other aspects dealing with the Soret and Dufour effects on steady boundary layer flow with combined heat transfer problems have been reported (2, 10, 38, 35, 1, 4, 20, 18).

Hall effect on MHD boundary layer flow over a continues semi-infinite flat plate moving with a uniform velocity in its own plane in an incompressible viscous and electrically conducting fluid in the presence of a uniform transverse magnetic field were investigated by Watanabe and Pop [41]. Abdallah [1] has analytic solution of heat and mass transfer over a permeable stretching plate affected by chemical reaction, internal heating, durous-soret effect and hall effect. The effect of Hall current on the study MHD flow of an electrically conducting, incompressible Burger's fluid between two parallel electrically insulating infinite plane was studied by Rana *et. al.* [32].

In all the above studies the physical situation is related to the process of uniform stretching sheet. For the development of more physically realistic characterization of the flow configuration it is very useful to introduce unsteadiness into the flow, heat transfer problems. The working fluid heat generation or absorption effects are very crucial in monitoring the heat transfer in the regions, heat removal from nuclear fuel debris, underground disposal of radioactive waste material, storage of food stuffs, exothermic chemical reactions and dissociating fluids in packed-bed reactors. This heat source can occurs in the form of a coil or battery. Very few studies have been found in literature on unsteady boundary flows over a stretching sheet by taking heat generation/absorption into the account. Wang [40] studied the unsteady boundary layer flow of a liquid film over a stretching sheet. Later, Elbashbeshy and Bazid [19] have presented the heat transfer over an unsteady stretching surface. Tsai *et al.* [39] have discussed flow and heat transfer characteristics over an unsteady stretching surface by taking heat source into the account. Ishak *et al.* [23] analyzed the effect of prescribed wall temperature on heat transfer flow over an unsteady stretching permeable surface. Ishak [24] has presented unsteady MHD flow and heat transfer behavior over a stretching plate. Recently, Dulal pal [16] has described the analysis of flow and heat transfer over an unsteady stretching surface with non-uniform heat source/sink and thermal radiation. Dulal pal *et al.* [17] has presented MHD non-Darcian mixed convection heat transfer over a non-linear stretching sheet with Soret–Dufour effects, heat source/sink and chemical reaction. Salem and Aziz [33] analysed the effect of Hall current and chemical reaction on the steady flow, heat transfer laminar of a viscous, electrically conducting fluid over a continuously stretching surface in the presence of heat generation/absorption. Aziz [8] investigated the flow and heat transfer of a viscous fluid flow over an unsteady stretching surface with Hall effects. Recently Sarojamma *et al.* (36, 37) have discussed the effect of Hall current on the flow induced by a stretching surface.

In this chapter, we study the combined influence of Hall effects and radiation absorption on unsteady convective heat transfer flow of a viscous electrically conducting fluid through a porous medium past a stretching sheet in the presence of non-uniform heat source.. The equations governing the flow of heat transfer have been solved by Galerkin finite element analysis with three nodded line segments.

## 2. FORMULATION OF THE PROBLEM:

We analyse the unsteady convective heat transfer flow of an electrically conducting fluid past a stretching sheet with the plane at y=0 and the flow is confined to the region y>0. A schematic representation of the physical model is exhibited in fig.1.We choose the frame of reference O(x,y,z) such that the x-axis is along the direction of motion of the surface, the y-axis is normal to the surface and z-axis transverse to the (x-y) plane. An uniform magnetic field of strength H0 is applied in the positive y-direction. The surface of the sheet is assumed to have a variable temperature $T_w(x)$, while the ambient fluid has a uniform temperature $T_\infty$, where $T_w(x) > T_\infty$ corresponds to a heated plate and $T_w(x) < T_\infty$, corresponds to a cooling plate. The effects of thermo-diffusion, thermal radiation, Hall currents, viscous dissipation are considered. We consider Hall effects into consideration and assume the electron pressure gradient, the ion-slip and the thermo-electric effects are negligible. Using boundary layer approximation, Boussinesq's approximation the basic equations governing the flow heat transfer is

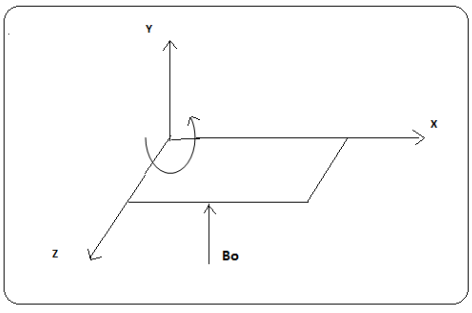

**Fig.1 : Physical Configuration of the Problem**

The equation of Continuity is

$$\frac{\partial u}{\partial x}+\frac{\partial v}{\partial y}=0 \tag{2.1}$$

 

The Momentum equations are

$$\frac{\partial u}{\partial t}+u\frac{\partial u}{\partial x}+v\frac{\partial u}{\partial y}=v\frac{\partial^2 u}{\partial y^2}+\beta g(T-T_\infty)-\left(\frac{\mu}{k}\right)u-\frac{\sigma B_0^2}{\rho(1+m^2)}(u+mw) \tag{2.2}$$

$$\frac{\partial w}{\partial t}+u\frac{\partial w}{\partial z}+v\frac{\partial w}{\partial z}=v\frac{\partial^2 w}{\partial y^2}-\left(\frac{\mu}{k}\right)v+\frac{\sigma B_0^2}{\rho(1+m^2)}(mu-w) \tag{2.3}$$

The energy equation is

$$\rho C_p\left(\frac{\partial T}{\partial t}+u\frac{\partial T}{\partial x}+v\frac{\partial T}{\partial y}\right)=k_f\frac{\partial^2 T}{\partial y^2}+q'''-\frac{\partial(q_R)}{\partial y}+\mu\left(\left(\left(\frac{\partial u}{\partial y}\right)^2+\left(\frac{\partial w}{\partial y}\right)\right)\right)^2+\frac{\sigma B_o^2(u^2+w^2)}{1+m^2} \tag{2.4}$$

The coefficient $q'''$ is the rate of internal heat generation (>0) or absorption (<0). The internal heat generation /absorption $q'''$ is modeled as

$$q'''=\left(\frac{ku_s}{x\nu}\right)\left[A1\left(T_w-T\infty\right)f'(\eta)+B1\left(T-T\infty\right)\right] \tag{2.5}$$

Where A1 and B1 are coefficients of space dependent and temperature dependent internal heat generation or absorption respectively. It is noted that the case A1>0 and B1>0, corresponds to internal heat generation and that A1<0 and B1<0, the case corresponds to internal heat absorption case.

The radiation heat term (Makinde [27] by using The Rosseland approximation is given by

$$q_r=-\frac{4\sigma^\bullet}{3\beta_R}\frac{\partial T'^4}{\partial y} \tag{2.6}$$

$$T'^4\cong 4TT_\infty^3-3T_\infty^4 \tag{2.7}$$

$$\frac{\partial q_R}{\partial z}=-\frac{16\sigma^\bullet T_\infty^3}{3\beta_R}\frac{\partial^2 T}{\partial y^2} \tag{2.8}$$

The non-dimensional temperature $\theta(\eta)=\dfrac{T-T_\infty}{T_w-T_\infty}$ can be simplified as

$$T=T_\infty(1+(\theta_w-1)\theta) \tag{2.9}$$

Where $\theta=\dfrac{T_w}{T_\infty}$ is the temperature parameter.

Using (2.5) & (2.9), equation (2.4) reduces to

$$\rho C_p\left(\frac{\partial T}{\partial t}+u\frac{\partial T}{\partial x}+v\frac{\partial T}{\partial y}\right)=k_f\frac{\partial^2 T}{\partial y^2}+q'''-\frac{\partial(q_R)}{\partial y}+\mu\left(\left(\frac{\partial u}{\partial y}\right)^2+\left(\frac{\partial w}{\partial y}\right)\right)^2+\frac{\sigma B_o^2(u^2+w^2)}{1+m^2} \tag{2.10}$$

where T is the temperature in the fluid. $k_f$ is the thermal conductivity, Cp is the specific heat at constant pressure, $\beta$ is the coefficient of thermal expansion, $q_r$ is the radiative heat flux, k is the porous permeability parameter.

The boundary conditions for this problem can be written as

$$u=U(x,t)+L\frac{\partial u}{\partial y},v=V_w(x,t),w=0,\frac{\partial T}{\partial y}=-\frac{q_w}{k_f}\quad on\quad y=0 \tag{2.11}$$

$$u=w=0,T=T_\infty\qquad as\ \ y\to\infty \tag{2.12}$$

Where u and v are the fluid velocity components along x and y-axis respectively and t is the time. $v_w(x,t)=-(\frac{\nu Uw}{x})^{1/2}f(0)$. The flow is caused by the stretching of the sheet which moves in its own plane with the

 

surface velocity $U_w(x,t)=\frac{ax}{(1-ct)}$, where a (stretching rate) and c are the positive constants having dimension time$^{-1}$ (with t < 1, c ≥ 0).It is noted that the stretching rate $\frac{a}{(1-ct)}$ increases with time, since a > 0. The surface temperature of the sheet varies with the distance *x* from the slot and time *t* in the form so that surface temperature $T_w(x,t)=T_\infty+\frac{ax^2}{2\nu(1-ct)^{3/2}}$ where a≥0 .The particular form of $U_w(x,t)$ and $T_w(x, t)$ has been chosen in order to derive a similarity transformation which transforms the governing partial differential equations (2.2), (2.3) and (2.10) into a set of highly nonlinear ordinary differential equations.

The radiation heat term (Brewester) by using the Rosseland approximation is given by

$$q_r=-\frac{4\sigma^{\bullet}}{3\beta_R}\frac{\partial T'^4}{\partial y} \tag{2.13}$$

$$T'^4\cong 4TT_\infty^3-3T_\infty^4 \tag{2.14}$$

$$\frac{\partial q_R}{\partial z}=-\frac{16\sigma^{\bullet}T_\infty^3}{3\beta_R}\frac{\partial^2 T}{\partial y^2} \tag{2.15}$$

The non-dimensional temperature $\theta(\eta)=\frac{T-T_\infty}{T_w-T_\infty}$ can be simplified as

$$T=T_\infty(1+(\theta_w-1)\theta)$$

Where $\theta=\frac{T_w}{T_\infty}$ is the temperature parameter.

The stream function ψ(x, t) is defined as:

$$u=\frac{\partial\psi}{\partial y}=\frac{ax}{(1-ct)}f'(\eta),v=-\frac{\partial\psi}{\partial x}=\frac{a\nu}{\sqrt{(1-ct)}}f(\eta) \tag{2.16}$$

we introduce the similarity variables (Dulal Pal [16]) as

$$\eta=\sqrt{\frac{a}{(1-ct)}}y \tag{2.17}$$

$$\psi(x,y,t)=\left(\frac{\nu a}{1-ct}\right)^{1/2}xf(\eta),w=\left(\frac{ax}{1-ct}\right)g(\eta) \tag{2.18}$$

$$T(x,t.t)=T_\infty+\frac{ax^2}{2\nu(1-ct)^{3/2}}\theta(\eta),\theta(\eta)=\frac{T-T_\infty}{T_w-T_\infty} \tag{2.19}$$

$$B^2=B_o^2(1-ct)^{-1} \tag{2.20}$$

Using equations (2.16) - (2.19) into equations (2.2), (2.3) and (2.10) we get

$$f'''+ff''-f'^2-S(f'+1.5f'')+G(\theta)-D^{-1}f'-\frac{M^2}{1+m^2}(mf'-g)=0 \tag{2.21}$$

$$g''+fg'-f'g-S(g'+1.5g'')-D^{-1}g+\frac{M^2}{1+m^2}(mf'-g)=0 \tag{2.22}$$

$$\begin{aligned}&Rd(1+(\theta_w-1)\theta)^3)\theta''+\Pr(f\theta'-2f'\theta-0.5S(3\theta+\eta\theta')+\Pr(A_1f'+B_1\theta)\\&+Ec((f'')^2+(g')^2)+\frac{M^2}{1+m^2}((f')^2+g^2)=0\end{aligned} \tag{2.23}$$

 

where S=c/a is the unsteadiness parameter. $M = \frac{\sigma B_0^2}{\rho a}$ is the magnetic parameter,

$D^{-1} = \frac{\nu}{ak}$ is the inverse Darcy parameter, $G = \frac{\beta g(T_w - T_\infty)}{U_w v_w^2}$ is the thermal buoyancy parameter, $\Pr = \frac{\mu C_p}{k_f}$ is the Prandtl number, $Ec = \frac{U_w^2}{C_P(T_w - T_\infty)}$ is the Eckert number, $m = \omega_e \tau_e$ is the Hall parameter $Rd = \frac{4\sigma^{\bullet} T_\infty^3}{\beta_R k_f}$ is the radiation parameter

The transformed boundary conditions (2.11) & (2.12) reduce to

$$f'(0) = 1 + A11 f''(0),\ f(0) = fw, g(0) = 0, \theta'(0) = -1 \tag{2.24}$$

$$f'(\infty) \to 0, g(\infty) \to 0, \theta(\infty) \to 0 \tag{2.25}$$

Where $fw = \frac{v_w}{\sqrt{av}}$ is the heat transfer coefficient such that fw>0 represents suction and fw<0 represents injection at the surface.

## 3. FINITE ELEMENT ANALYSIS

The method basically involves the following steps:

(1) Division of the domain into elements, called the finite element mesh.
(2) Generation of the element equations using variational formulations.
(3) Assembly of element equations as in step 2.
(4) Imposition of boundary conditions to the equations obtained in step 3
(5) Solution of the assumed algebraic equations.

The assumed equations can be solved by any of the numerical technique viz. Gaussian elimination, LU Decomposition method etc.

**VARIATIONAL FORMULATION**: The variational form associated with the equations (2.21)-(2.23) over a typical two nodded line at element $(\eta_e, \eta_{e+1})$ is given by

$$\int_{\eta_e}^{\eta_{e+1}} w_1 (f' - h) d\eta = 0 \tag{3.1}$$

$$\int_{\eta}^{\eta_{e+1}} w_{12} (h'' + fh' - h^2 - S(h + 1.5h') + G(\theta) - \frac{M^2}{1+m^2}(h + mg)) d\eta = 0 \tag{3.2}$$

$$\int_{\eta_e}^{\eta_{e+1}} w_3 (g'' + fg' - S(g' + 1.5g'') - (h + \frac{M^2}{1+m^2})g + \frac{mM^2}{1+m^2} h) d\eta = 0 \tag{3.3}$$

$$\int_{\eta e}^{\eta e+1} w_4 (Rd(1 + (\theta_w - 1)\theta)^3)\theta'' + \Pr(f\theta' - 2f'\theta - 0.5S(3\theta + \eta\theta') + \Pr(A_1 f' + B_1\theta) + Ec((f'')^2 + (g')^2) + \frac{M^2}{1+m^2}(f')^2 + g^2) d\eta = 0 \tag{3.4}$$

Where w1, w2, w3, w4, w5 are arbitrary test functions and may be regarded as the variations in f, h, g, θ and $\phi$ respectively.

## FINITE ELEMENT FORMULATION

The finite element method may be obtained from (3.1)-(3.4) by substituting finite element approximations of the form

$$f = \sum_{k=1}^{3} f_k \psi_k,\ h = \sum_{k=1}^{3} h_k \psi_k,\ g = \sum_{k=1}^{3} g_k \psi_k,\ \theta = \sum_{k=1}^{3} \theta_k \psi_k \tag{3.5}$$

We take w1=w2=w3=w4= $\psi_i^j$ $(i, j = 1,2,3)$ (3.6)

 

Using (3.6) we can write equations (3.1) - (3.4) as

$$\int_{\eta_e}^{\eta_{e+1}} \left( \frac{df}{d\eta} - h \right) \psi_i^j \, d\eta = 0 \tag{3.7}$$

$$\int_{\eta_e}^{\eta_{e+1}} \left( \frac{d}{d\eta}\left(\frac{dh}{d\eta}\right) + f\left(\frac{dh}{d\eta}\right) - h^2 - S(h + 1.5h') + G(\theta) - \frac{M^2}{1+m^2}(h + mg) \right) \psi_i^j \, d\eta = 0 \tag{3.8}$$

$$\int_{\eta_e}^{\eta_{e+1}} \left( \frac{d}{d\eta}\left(\frac{dg}{d\eta}\right) + f\left(\frac{dg}{d\eta}\right) - S\left(\frac{dg}{d\eta} + 1.5\frac{d}{d\eta}\left(\frac{dg}{d\eta}\right) - \left(h + \frac{M^2}{1+m^2}\right)\right) g + \frac{mM^2}{1+m^2} h \right) \psi_i^j \, d\eta = 0 \tag{3.9}$$

$$\int_{\eta e}^{\eta e+1} \left( \frac{d}{d\eta}\left(\frac{d\theta}{d\eta}\right) Rd(1 + (\theta_w - 1)\theta)^3 \right) + \Pr(f\theta' - 2f'\theta - 0.5S(3\theta + \eta\theta') + \Pr(A_1 f' + B_1\theta) + \\ + \Pr Ec((f'')^2 + (g')^2) + \frac{\Pr EcM^2}{1+m^2}((f')^2 + g^2) \, d\eta = 0 \tag{3.10}$$

Following Galerkin weighted residual method and integration by parts method the equations (3.7)-(3.10) we obtain

$$\int_{\eta_e}^{\eta_{e+1}} \left( \frac{df}{d\eta} - h \right) \psi_i^j \, d\eta = 0 \tag{3.11}$$

$$\int_{\eta_e}^{\eta_{e+1}} \frac{d\psi_i^j}{d\eta}\left(\frac{dh}{d\eta}\right) d\eta - \int_{\eta_e}^{\eta_{e+1}} f\left(\frac{dh}{d\eta}\right)\psi_i^j \, d\eta + \int_{\eta_e}^{\eta_{e+1}} h^2 \psi_i^j \, d\eta - S\int_{\eta_e}^{\eta_{e+1}} \left(h + 1.5\frac{dh}{d\eta}\right) d\eta$$

$$- G\int_{\eta_e}^{\eta_{e+1}} (\theta)\psi_i^j \, d\eta + \frac{M^2}{1+m^2}\int_{\eta_e}^{\eta_{e+1}} (h + mg)\psi_i^j \, d\eta = Q_{1,j} + Q_{2,j}$$

$$- Q_{1,jj}\psi_j(\eta_e)\left(\frac{dh}{d\eta}\right)(\eta_e) \quad Q_{2,jj}\psi_j(\eta_{e+1e})\left(\frac{dh}{d\eta}\right)(\eta_{e+1e}) \tag{3.12}$$

$$\int_{\eta_e}^{\eta_{e+1}} \frac{d\psi_i^j}{d\eta}\frac{dg}{d\eta} d\eta - \int_{\eta_e}^{\eta_{e+1}} f\left(\frac{dg}{d\eta}\right)\psi_i^j d\eta + \int_{\eta_e}^{\eta_{e+1}} \left(\left(h + \frac{M^2}{1+m^2}\right)g + \frac{mM^2}{1+m^2}\right)\psi_i^j d\eta - S\int_{\eta_e}^{\eta_{e+1}} \left(\frac{dg}{d\eta} + 1.5\frac{d}{d\eta}\left(\frac{dg}{d\eta}\right)\right) d\eta = R_{1,j} + R_{2,j} \tag{3.13}$$

*where*

$$-R_{1,j} = \psi_j(\eta_e)\frac{dg}{d\eta}(\eta_e) \qquad R_{2,j} = \psi_j(\eta_{e+1})\frac{dg}{d\eta}(\eta_{e+1})$$

$$\int_{\eta e}^{\eta e+1} \frac{d\psi}{d\eta}\left(\frac{d\theta}{d\eta}\right) Rd(1 + (\theta_w - 1)\theta)^3) + \Pr\int_{\eta e}^{\eta_{e+1}} \left(f\frac{d\theta}{d\eta} - 2\frac{df}{d\eta}\theta - 0.5S(3\theta + \eta\theta')\psi_j^i d\eta + \Pr\int_{\eta_e}^{\eta_{e+1}} (A_1 f' + B_1\theta)\psi_j^i d\eta + \right.$$

$$\left. + Ec\int_{\eta_e}^{\eta_{e+1}} ((f'')^2 + (g')^2) + \frac{M^2}{1+m^2}((f')^2 + g^2))\psi_j^i d\eta = 0 \right.$$

$$--S_{1,j} = \psi_j(\eta_e)\frac{d\theta}{d\eta}(\eta_e) \;, \quad S_{2,j} = \psi_j(\eta_{e+})\frac{d\theta}{d\eta}(\eta_{e+1}) \tag{3.14}$$

Expressing $f^k, h^k, \theta^k$ in terms of local nodal values (3.12)-(3.15) we obtain

$$\sum_{k=1}^{3} h^k \int_{\eta_e}^{\eta_{e+1}} \frac{d\psi_i^j}{d\eta}\left(\frac{dh}{d\eta}\right) d\eta - \sum_{k=1}^{3} f^k \int_{\eta_e}^{\eta_{e+1}} \psi^k \left(\frac{dh}{d\eta}\right)\psi_i^j d\eta + \sum_{k=1}^{3} (h^{k2}) \int_{\eta_e}^{\eta_{e+1}} \psi_k^2 \psi_i^j d\eta$$

$$- S\sum_{k=1}^{3} h^k \left( \int_{\eta_e}^{\eta_{e+1}} \left(\psi_k + 1.5\frac{d\psi_k}{d\eta}\right)\psi_i^j d\eta - G\sum_{k=1}^{3} \int_{\eta_e}^{\eta_{e+1}} (\theta^k)\psi_k\psi_i^j d\eta \right.$$

$$+ \frac{M^2}{1+m^2}\sum_{k=1}^{3} \int_{\eta_e}^{\eta_{e+1}} (h^k + mg^2)\psi_k\psi_i^j d\eta = Q_{1,j} + Q_{2,j}$$

Where

$$- Q_{1,jj}\psi_j(\eta_e)\left(\frac{dh}{d\eta}\right)(\eta_e) \quad Q_{2,jj}\psi_j(\eta_{e+1e})\left(\frac{dh}{d\eta}\right)(\eta_{e+1e}) \tag{3.17}$$

 

$$\sum_{k=1}^{3} g^k \int_{\eta_e}^{\eta_{e+1}} \frac{d\psi_i^j}{d\eta}\frac{d\psi_k}{d\eta}d\eta - \sum_{k=}^{3} f^k g^k \int_{\eta_e}^{\eta_{e+1}} (\frac{d\psi_k}{d\eta})\psi_k\psi_i^j d\eta +$$
$$-S\sum_{k=1}^{3} g^k (\int_{\eta_e}^{\eta_{e+1}} (\psi_k + 1.5\frac{d\psi_k}{d\eta})\psi_i^j\, d\eta + \sum_{k=1}^{3}\int_{\eta_e}^{\eta_{e+1}} ((h^k + \frac{M^{32}}{1+m^2})g^k + \frac{mM^2}{1+m^2}h^k)\psi_k\psi_i^j d\eta = R_{1,j} + R_{2,j}$$

*where*

$$-R_{1,j} = \psi_j(\eta_e)\frac{dg}{d\eta}(\eta_e) \qquad R_{2,j} = \psi_j(\eta_{e+1})\frac{dg}{d\eta}(\eta_{e+1}) \tag{3.18}$$

$$\left(\frac{d\psi}{d\eta}\frac{d\psi_k}{d\eta}d\eta + \Pr\sum^{3}\int_{\eta_e}^{\eta_{e+1}} f^k\left(\frac{d\theta^k}{d\eta}\right)\right)\psi_k\psi_i^j d\eta - \sum^{3}\int_{\eta_e}^{\eta_{e+1}} \varphi^k\psi_k d\eta$$
$$\sum_{k=1}^{3}\theta^k\int_{\eta_e}^{\eta_{e+1}} P_r A1\sum_{1}^{3} h''\int_{\eta_e}^{\eta_e+1}\psi_i^j\psi_i^k d\eta - P_r B1\sum_{1}^{3}\theta''\int_{\eta_e}^{\eta_e+1}\psi_i^j\psi_i^k d\eta + Ec\sum\int_{\eta_e}^{\eta_e+1}(h_k\psi_k)^2\psi_i^j d\eta$$
$$+\frac{M^2 Ec}{1+m^2}\sum\int_{\eta_e}^{\eta_e+1}(g_k\psi_k)^2\psi_k d\eta - P_r\sum_{\eta_e}^{3}\int^{\eta_{e+1}}\theta^k(\frac{df^k}{d\eta}))\psi_k\psi_i^j d\eta - 0.5SP_r\sum_{\eta_e}^{3}\int^{\eta_{e+1}}\theta^k(3+\eta\frac{d\psi_k}{d\eta}))\psi_i^j d\eta = S_{1,j} + S_{2,j} \tag{3.19}$$

*where*

$$-S_{1,j} = \psi_j(\eta_e)\frac{d\theta}{d\eta}(\eta_e)k = 1 \qquad S_{2,j} = \psi_j(\eta_{e+1})\frac{d\theta}{d\eta}(\eta_{e+1})$$

Choosing different $\psi_{i\,j}^{\,j}$ corresponding to each element $\eta_e$ in the equation (3.16) yields a local stiffness matrix of order 3x3 in the form

$$(f_{i,j}^k)(1-2R)u_i^k - G(\theta_i^k) + \frac{M^2}{1+m^2}(g_i^k) = (Q_{1,j}^k) + (Q_{2,j}^k) \tag{3.20}$$

Likewise the equations (3.17), (3.18) & (3.19) give rise to a stiffness matrices

$$(g_{i,j}^k) + (1+2R)(f_i^k) - \frac{mM^2}{1+m^2}(u_i^k) = (R_{1,j}^k) + (R_{2,j}^k) \tag{3.21}$$

$$(e_{i,j}^k)(1+\Pr B^*)(\theta_i^k) - P_r(u_i^k) - P_r A^*\left(m_{i,j}^k\right) = (S_{1,j}^k) + (S_{2,j}^k) \tag{3.22}$$

where $(f_{i,j}^k),(g_{i,j}^k),(\theta_{i,j}^k),(e_{i,j}^k),(l_{i,j}^k),\left(m_{i,j}^k\right),(n_{i,j}^k)$ are 3x3 matrices and $.(Q_{1,jj}^k),(Q_{2,jj}^k),(R_{1,jj}^k),(R_{1,jj}^k),(S_{1,jj}^k)\,and\,(S_{1,jj}^k)$ are 3x1 column matrices and such stiffness matrices (3.21)-(3.22) in terms of local nodes in each element are assembled using inter element continuity and equilibrium conditions to obtain the coupled global matrices in terms of the global node values of h, f and g. In case we choose n quadratic elements then the global matrices are of order 2n+1.The ultimate coupled global matrices are solved to determine the unknown global values of velocity, temperature in the fluid region. In solving these matrices an iteration procedure has been adopted.

The shape functions are

$$\psi_i^i = \frac{(y-8)(y-16)}{128} \qquad \psi_2^1 = \frac{(y-24)(y-32)}{128} \qquad \psi_3^1 = \frac{(y-40)(y-48)}{128}$$
$$\psi_i^{2i} = \frac{(y-4)(y-8)}{32} \qquad \psi_2^2 = \frac{(y-12)(y-16)}{32} \qquad \psi_3^2 = \frac{(y-20)(y-24)}{128}$$
$$\psi_i^3 = \frac{(3y-8)(3y-16)}{128} \quad \psi_2^3 = \frac{(3y-24)(3y-32)}{128} \quad \psi_3^3 = \frac{(3y-40)(3y-48)}{128}$$
$$\psi_i^4 = \frac{(y-2)(3y-4)}{8} \quad \psi_2^4 = \frac{(y-6)(y-8)}{8} \qquad \psi_3^4 = \frac{(y-10)(y-12)}{8}$$
$$\psi_i^5 = \frac{(5y-8)(5y-16)}{128} \quad \psi_2^5 = \frac{(5y-24)(5y-32)}{128} \quad \psi_3^5 = \frac{(5y-40)(5y-48)}{128}$$

**4. STIFFNESS MATRICES**

The global matrix for θ is $A_3X_3=B_3$
The global matrix for h is $A_4X_4=B_4$
The global matrix for f is $A_5X_5=B_5$
The global matrix for g is $A_6X_6=B_6$

 

## 5. SKIN FRICTION and NUSSELT NUMBER

The physical quantities of engineering interest in this problem are the skin friction coefficient Cf, the Local Nusselt number Nux which are expressed as

$$\frac{1}{2}C_f\sqrt{R_{ex}} = f''(0),\ \frac{1}{2}C_{fz}\sqrt{R_{ez}} = g'(0), \qquad Nux/\sqrt{R_{ex}} = 1/\theta(0)$$

Where $\mu = \dfrac{k}{\rho C_p}$ is the dynamic viscosity of the fluid and Rex is the Reynolds number.

For the computational purpose and without loss of generality $\infty$ has been fixed as $\eta_{max}$=8.The whole domain is divided into 11 line elements of equal width, each element being three nodded.

**COMPARISON:** Comparison of Nu(0) for M=m=G=Ec= fw, A1=B1=0, θw=0, A=A11=0

| Pr | Chen(14a) | Grubka and Bobba (20a) | Aziz(18a) | Sarojamma et al (37) | Present results |
|---|---|---|---|---|---|
| 0.01 | 0.02942 | 0.0294 | 0.02948 | 0.02949 | 0.029479 |
| 0.72 | 1.08853 | 1.0885 | 1.08855 | 1.08857 | 1.088559 |
| 1.0 | 1.33334 | 1.3333 | 1.33333 | 1.33335 | 1.333329 |
| 3.0 | 2.50972 | 2.5097 | 2.50972 | 2.50974 | 2.509736 |
| 7.0 | 3.97150 | | 3.97151 | 3.97152 | 3.971519 |
| 10.0 | 4.79686 | 4.7969 | 4.79687 | 4.79688 | 4.796869 |
| 100.0 | 15.7118 | 15.712 | 15.7120 | 15.7122 | 15.71212 |

## 6. DISCUSSION OF THE NUMERICAL RESULTS

In order to validate the accuracy of the numerical scheme employed we have compared the local temperature gradient of the present analysis with those of Chen (15). Grubka and Bobba (20a), Aziz(8) and Sarojamma *et al.* (36) for different values of Prandtl number in absence of magnetic field, thermal and solutal buoyancy, radiation absorption, viscous dissipation, temperature parameter and suction for steady flow M=Gr= Ec= fw=A1=B1=0 = θw =0 =A11=0 and presented in table.1 and are found to be in good agreement.

Figs.2 a-2c represents the velocity, temperature wit Hall parameter (m). As mentioned above the Lorentz force has a retarding effect on the primary velocity, this retardation is enhanced with increase in the Hall parameter and hence the primary velocity is enhanced and consequently the momentum boundary layers become thicker. The secondary velocity increases as the Hall parameter increases. The effect of Hall parameter on temperature shows that the temperature reduces with increase in Hall parameter (m). This is due to the reduction of thermal boundary layer.

Figs.3a-3c represent the impact of thermal radiation on the velocities, temperature. It can be seen from the profiles that higher the radiative heat flux, larger the velocities, temperature. This is due to the fact that the thickness of the momentum and thermal boundary layers with increase in the radiation parameter (Nr).

Figs.4a-4c show the variation of velocity, temperature with Eckert number (Ec). It is pointed out that the presence of Eckert number enhances the primary and secondary velocity components. This is due to the fact that the energy is generated in the fluid. An increase in Ec increases the temperature. This is owing to the fact that the thermal energy is generated in the fluid on account of frictional heating. Hence, the temperature distribution rises in the entire thermal boundary layer.

Figs.5a-5c and 6a-6d represent the velocity, temperature with space dependent heat source and temperature dependent source. An increase in the space dependent source (A1>0) enhances the velocities, temperature owing to the generation of energy in the boundary layer while in the case of heat absorption source (A1<0), the primary, secondary velocities, the temperature reduce in the boundary layer. In the case of temperature dependent generating source (B1>0), the velocities, temperature enhance and for B1<0, it reduces in the flow region.

Figs.7a-7c represent the velocity, temperature with unsteady parameter S. It can be seen from the profiles that an increase in S reduces the primary velocity in the entire flow region, while the secondary velocity reduces with S in the region(0,2.5) and enhances in the remaining flow region. This is due to the fact that the thickness of the momentum boundary layer reduces with increase in unsteady parameter S. The variation of θ with S shows that the thickness of thermal boundary layer increases with increasing S.

 

Fig.8a-8c represent the effect of slip parameter (A11) on the velocities, temperature. From the profiles we find that the primary velocity reduces with slip parameter (A11) in the entire region. The secondary velocity reduces in the flow region (0, 2.0) and enhances in the remaining region. An increase in A11 increases the temperature in the entire flow region.

Figs.9a-9c illustrate the variation of velocities, temperature with temperature parameter (A). Higher the values of temperature parameter (A≤1.5) smaller the velocities, temperature in the boundary layer and for higher A≥2.0, we notice an enhancement in velocities, temperature in the flow region. Thus the non-linearity of thermal radiation leads to a reduction in velocities, temperature.

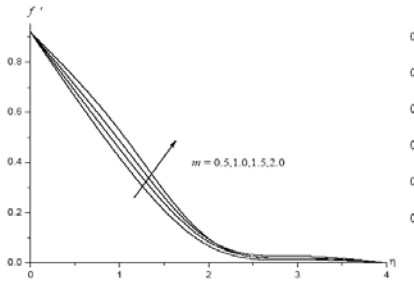


Fig.2a Effect of m on $f'$ (η)
S=0.1, A1=0.1, B1=0.1,
Nr=0.5, A11= 0.2, A=0.2, Ec=1.3

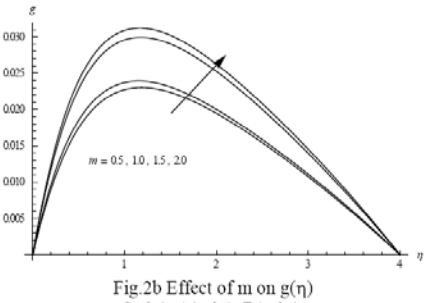


Fig.2b Effect of m on g(η)
S=0.1, A1=0.1, B1=0.1,
Nr=0.5, A11= 0.2, A=0.2, Ec=1.3

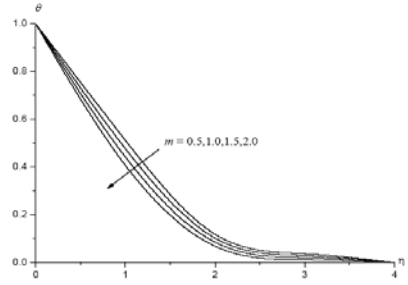


Fig.2c Effect of m on θ(η)
S=0.1, A1=0.1, B1=0.1,
Nr=0.5, A11= 0.2, A=0.2, Ec=1.3

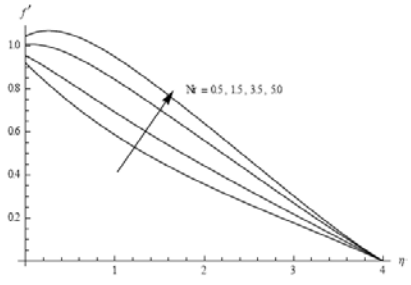


Fig.3a Effect of Nr on $f'$ (η)
m=0.5, S=0.1, A1=0.1, B1=0.1,
A11= 0.2, A=0.2, Ec=1.3

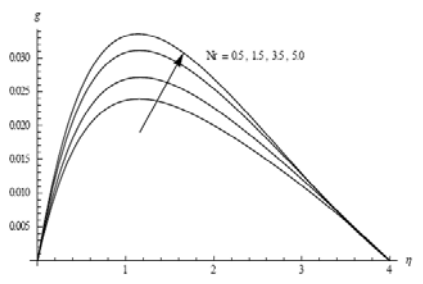


Fig.3b Effect of Nr on g(η)
m=0.5, S=0.1, A1=0.1, B1=0.1,
A11= 0.2, A=0.2, Ec=1.3

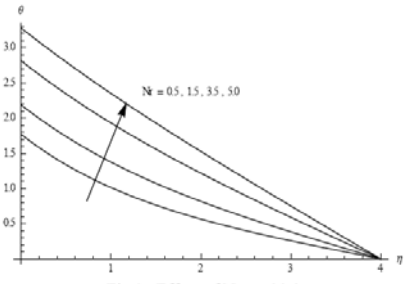


Fig.3c Effect of Nr on θ(η)
m=0.5, S=0.1, A1=0.1, B1=0.1,
A11= 0.2, A=0.2, Ec=1.3

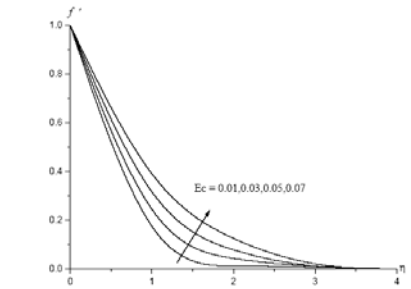


Fig.4a Effect of Ec on $f'$ (η)
m=0.5, S=0.1, A1=0.1, B1=0.1,
Nr=0.5, A11= 0.2, A=0.2

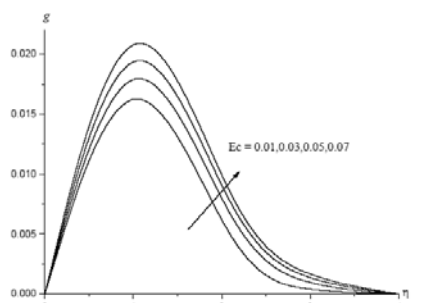


Fig.4b Effect of Ec on g(η)
m=0.5, S=0.1, A1=0.1, B1=0.1,
Nr=0.5, A11= 0.2, A=0.2

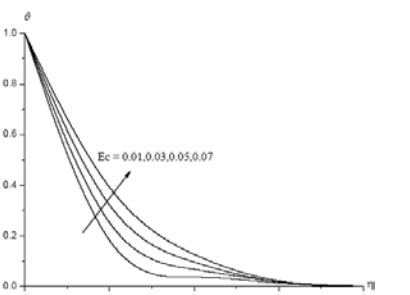


Fig.4c Effect of Ec on θ(η)
m=0.5, S=0.1, A1=0.1, B1=0.1,
Nr=0.5, A11= 0.2, A=0.2

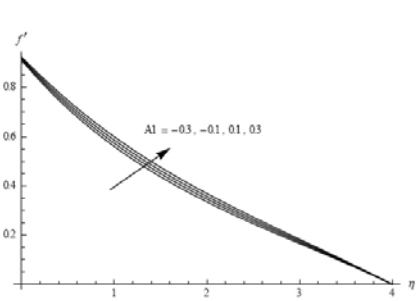


Fig.5a Effect of A1 on $f'$ (η)
m=0.5, S=0.1, A11=0.2, B1=0.1,
Nr=0.5, A=0.2, Ec=1.3

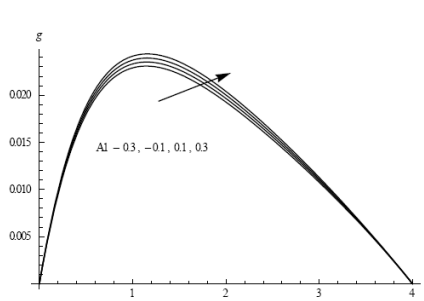


Fig.5b Effect of A1 on g(η)
m=0.5, S=0.1, A11=0.2, B1=0.1,
Nr=0.5, A=0.2, Ec=1.3

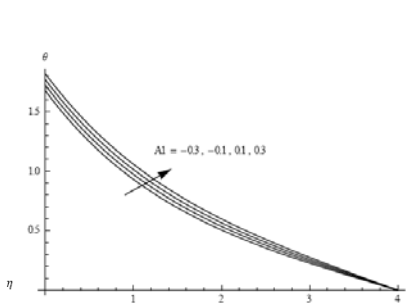


Fig.5c Effect of A1 on θ(η)
m=0.5, S=0.1, A11=0.2, B1=0.1,
Nr=0.5, A=0.2, Ec=1.3

 

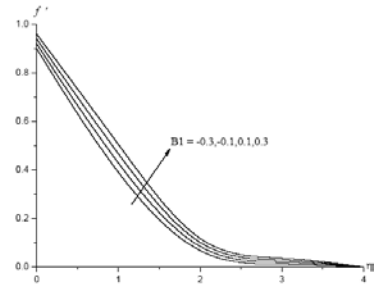


Fig.6a Effect of B1 on $f'(\eta)$
m=0.5, S=0.1, A1=0.1,
Nr=0.5, A11= 0.2, A=0.2, Ec=1.3

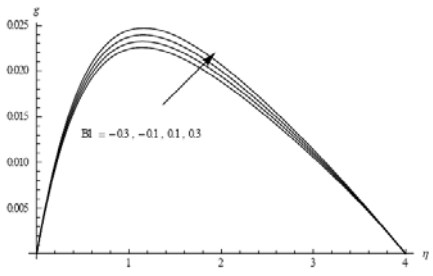


Fig.6b Effect of B1 on g(η)
m=0.5, S=0.1, A1=0.1,
Nr=0.5, A11= 0.2, A=0.2, Ec=1.3

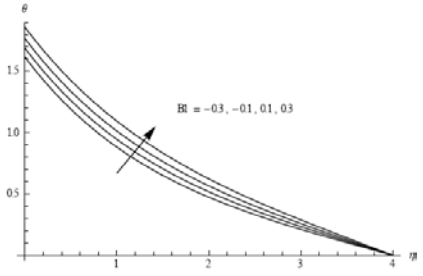


Fig.6c Effect of B1 on θ(η)
m=0.5, S=0.1, A1=0.1,
Nr=0.5, A11= 0.2, A=0.2, Ec=1.3

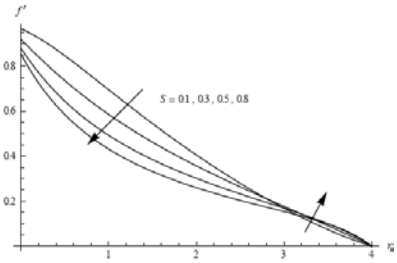


Fig.7a Effect of $S$ on $f'(\eta)$
m=0.5, A1=0.1, B1=0.1,
Nr=0.5, A11= 0.2, A=0.2, Ec=1.3

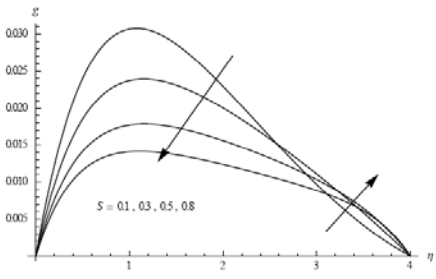


Fig.7b Effect of $S$ on g(η)
m=0.5, A1=0.1, B1=0.1,
Nr=0.5, A11= 0.2, A=0.2, Ec=1.3

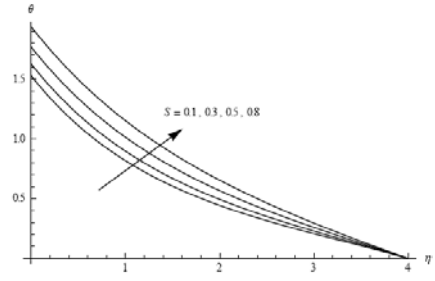


Fig.7c Effect of $S$ on θ(η)
m=0.5, A1=0.1, B1=0.1,
Nr=0.5, A11= 0.2, A=0.2, Ec=1.3

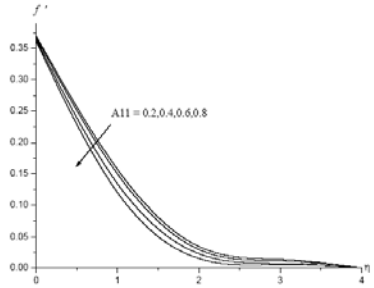


Fig.8a Effect of A11 on $f'(\eta)$
m=0.5, S=0.1, A1=0.1, B1=0.1,
Nr=0.5, A=0.2, Ec=1.3

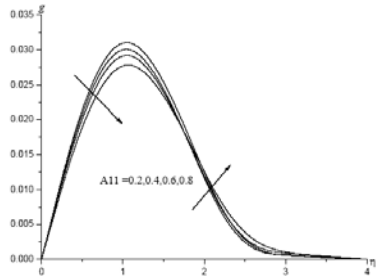


Fig.8b Effect of A11 on g(η)
m=0.5, S=0.1, A1=0.1, B1=0.1,
Nr=0.5, A=0.2, Ec=1.3

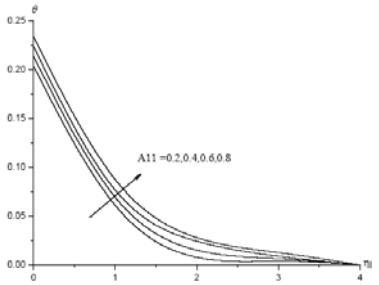


Fig.8c Effect of A11 on θ(η)
m=0.5, S=0.1, A1=0.1, B1=0.1,
Nr=0.5, A=0.2, Ec=1.3

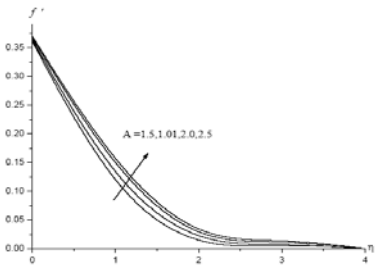


Fig.9a Effect of A on $f'(\eta)$
m=0.5, S=0.1, A1=0.1, B1=0.1,
Nr=0.5, A11= 0.2, Ec=1.3

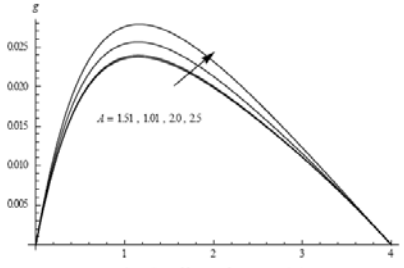


Fig.9b Effect of A on g(η)
m=0.5, S=0.1, A1=0.1, B1=0.1,
Nr=0.5, A11= 0.2, Ec=1.3

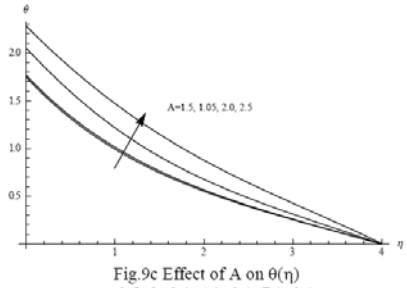


Fig.9c Effect of A on θ(η)
m=0.5, S=0.1, A1=0.1, B1=0.1,
Nr=0.5, A11= 0.2, Ec=1.3

**Table – 2:** Skin friction, Nusselt number at η=0

| Parameter | | τx(0) | τz(0) | Nu(0) |
|---|---|---|---|---|
| **m** | 0.5 | -0.404281 | 0.058909 | 0.565719 |
| | 1 | -0.391572 | 0.0718493 | 0.566888 |
| | 1.5 | -0.363934 | 0.0715603 | 0.569485 |
| | 2 | -0.349105 | 0.0544777 | 0.570909 |
| **A1** | 0.1 | -0.404281 | 0.058909 | 0.565719 |
| | 0.3 | -0.382347 | 0.059674 | 0.550298 |
| | -0.1 | -0.424696 | 0.058191 | 0.580827 |
| | -0.3 | -0.445637 | 0.0574487 | 0.597143 |
| **B1** | 0.1 | -0.404281 | 0.058909 | 0.565719 |
| | 0.3 | -0.363964 | 0.060293 | 0.537686 |
| | -0.1 | -0.438645 | 0.0577126 | 0.591893 |

 

| Parameter | | τx(0) | τz(0) | Nu(0) |
|---|---|---|---|---|
| | -0.3 | -0.471073 | 0.0565699 | 0.618806 |
| Nr | 0.5 | -0.404281 | 0.058909 | 0.565719 |
| | 1.5 | -0.225458 | 0.0648081 | 0.457641 |
| | 3.5 | 0.0345795 | 0.0727485 | 0.355834 |
| | 5 | 0.221987 | 0.0780472 | 0.305255 |
| Ec | 0.01 | -0.404281 | 0.058909 | 0.565719 |
| | 0.03 | -0.402784 | 0.0589593 | 0.564633 |
| | 0.06 | -0.40196 | 0.0589871 | 0.563986 |
| | 0.07 | -0.399854 | 0.059058 | 0.562423 |
| S | 0.1 | -0.404281 | 0.058909 | 0.565719 |
| | 0.3 | -0.602118 | 0.0476791 | 0.615421 |
| | 0.5 | -0.486037 | 0.0249963 | 0.653827 |
| | 0.7 | -0.0202435 | 0.00339035 | 2.46159 |
| A | 1.01 | -0.404281 | 0.058909 | 0.565719 |
| | 1.5 | -0.414303 | 0.0585557 | 0.572582 |
| | 2.0 | -0.292712 | 0.062304 | 0.487525 |
| | 2.5 | -0.181817 | 0.0662635 | 0.438195 |
| A11 | 0.2 | -0.404281 | 0.058909 | 0.565719 |
| | 0.4 | -0.307205 | 0.0574862 | 0.561963 |
| | 0.6 | -0.252386 | 0.0566687 | 0.559805 |
| | 0.8 | -0.214252 | 0.0560938 | 0.558289 |

The skin friction coefficients ($\tau_x$) and ($\tau_z$) are exhibited in table.2 for different values of m, Ec, S, A, A1, A11, B1, and Nr. An increase in the Hall parameter (m) reduces τx and enhances τy at the wall η=0. The variation of stress with radiation parameter (Nr) shows that τx reduces with increase in Nr≤3.5 and enhances with higher values of Nr≥5.0, while τy increases with higher radiative heat flux on the wall. Higher the dissipative heat smaller τx and larger $\tau_Y$ at the wall. An increase in space dependent/temperature dependent heat generating source reduces τx for A1 (>0) or B1 (>0) and enhances with A1<0 or B1<0. τy enhances at the wall with A1>0 or B1>0 while a reversed effect is noticed at the wall for A<0 or B1<0. The variation of stress components with temperature parameter (A) shows that an increases in A≤1.5 enhances τx and reduces $\tau_y$ and for still higher A≥2.0, a reversed effect is noticed in their behaviour. Thus the non-linearity in thermal radiation leads to an enhancement in the stress component $\tau_y$ and reduction in τy at the wall for smaller values of A and for higher values of A ,τx reduces and τy enhances at the wall. With respect to the partial slip(A11),we find that both the stress components reduce on the wall η=0.

The rate of heat transfer (Nusselt number) at the wall η=0 is exhibited in table.2.for different parametric variations. It is found that the rate of heat transfer increases with Hall parameter (m). Higher the dissipative energy (Ec) or thermal radiation(Nr) smaller Nu on the wall. $|Nu|$ decreases with increase in the space dependent/ temperature dependent heat source and for A1<0 or B1<0, Nu enhances on the wall. The effect of unsteady parameter S is to enhance the rate of heat transfer on the wall. The rate of heat transfer at the wall enhances with increase in temperature parameter A≤1.5 and reduces with higher values of A ≥2.0.Thus non-linearity in thermal radiation leads to an enhancement in Nu for smaller values of A and reduces for higher values of A. With respect to slip parameter (A11), we find that the Nusselt number reduces on the wall.

## 7. CONCLUSIONS

The coupled equations governing the flow heat transfer have been solved by employing Finite element method. The velocity, temperature is discussed graphically for different variations. The conclusions of this analysis are:

- An increase in Hall parameter (m) reduces the primary and secondary velocities, temperature reduces. The stress component τx enhances, Nusselt number and the stress component τy reduce at the wall.
- The primary, secondary velocities, temperature enhance reduces with increase in A1>0 while they experience a reduction with A1<0.An increase in B1>0 reduces the velocities, enhances the temperature. A reversed effect is notices with B1<0.
- The velocity components, the temperature enhances, reduces with increase in Nr. The rate of heat transfer enhances while the Sherwood number reduces at the wall.
- Higher the dissipation smaller the velocities, and smaller temperature. The, stress component τy and rate of heat transfer, reduces, the secondary velocity,τx enhances on the wall.
- An increase in Unsteady parameter S reduces the velocities, reduces the temperature and in the flow region. The stress component τx and Nusselt number reduces on the wall.

 

## 8. REFERENCES

1. Abdallah, I. A.: Analytic solution of heat and mass transfer over a permeable stretching plate affected by chemical reaction. Internal heating, Dufour-Soret effect and Hall effect, Therm. Sci.13 (2), 183–197. (2009).
2. Afify, A.A: MHD free-convective flow and mass transfer over a stretching sheet with chemical reaction. Int. J. Heat Mass transfer. Vol.40, pp.495-500 (2004).
3. Afify, A. A: Similarity solution in MHD: Effects of thermal diffusion and diffusion thermo on free convective heat and mass transfer over a stretching surface considering suction or injection, Commun. Nonlinear. Sci. Numer. Simul., 14, 2202–2214. (2009).
4. Alam, M. S., and Rahman, M. M: Dufour and Soret effects on mixed convection flow past a vertical porous flat plate with variable suction, Nonlinear Anal. Model. Control, 11, 3–12. (2006).
5. Alam, M. S., Ferdows, M. S., Ota, M., and Maleque, M. A.: Dufour and Soret effects on steady free convection and mass transfer flow past a semi-infinite vertical porous plate in a porous medium, Int. J. Appl. Mech. Eng.,11(3), 535–545(2006).
6. Alam, M. S., Rahman, M. M., Ferdows, M., Kaino, K., Mureithi, E., and Postelnicu, A: Diffusion-thermo and thermal-diffusion effects on free convective heat and mass transfer flow in a porous medium with time dependent temperature and concentration, Int. J. Appl. Eng. Res.,2(1), 81–96.(2007).
7. Anghel, M., Takhar, H. S., and Pop, I: Dufour and Soret effects on free convection boundary-layer over a vertical surface embedded in a porous medium, Stud. Univ. Babes-Bolyai Math., 45(4), 11–21 (2000).
8. Aziz,M.A.E: Flow and heat transfer over a unsteady stretching surface with Hall effects., Mechanica, V.45, pp.97-109(2010).
9. Beg, O. A., Bakier, A. Y., and Prasad, V. R: Numerical study of free convection magnetohydrodynamic heat and mass transfer from a stretching surface to a saturated porous medium with Soret and Dufour effects, Comput. Mater. Sci., 46, 57–65 (2009).
10. Chamkha, A. J., and Ben-Nakhi, A: MHD mixed convection-radiation interaction along a permeable surface immersed in a porous medium in the presence of Soret and Dufour's effect, Heat Mass Transfer,44, 845–856 (2008).
11. Chamkha, A. J., and Khaled, A. A.-R: Hydromagnetic combined heat and mass transfer by natural convection from a permeable surface embedded in a fluid saturated porous medium, Int. J. Numer. Methods Heat Fluid Flow, 10 (5), 455–476 (2000).
12. Chandrasekhara, B. C., Radha, N., and Kumari, M: The effect of surface mass transfer on buoyancy induced flow in a variable porosity medium adjacent to a vertical heated plate, Heat Mass Transfer, 27(3), 157–166 (1992).
13. Chapman, S., and Cowling, T. G: (1952).The Mathematical Theory of Non-uniform Gases, 2nded., Cambridge Univ. Press, Cambridge (1952).
14. Chen C.H: Laminar mixed convection adjacent to vertical continuously stretching sheets, Heat and Mass transfer, V.33, pp.471-476(1998).
15. Cheng, P: Two dimensional radiating gas flow by a moment method, AIAA J. 2(9), 1662–1664. (1964).
16. Dulal Pal: Combined effects of non-uniform heat source/sink and thermal radiation on heat transfer over an unsteady stretching permeable surface, Commun Nonlinear SciNumer Simulat, 16, 1890–1904, (2011).
17. Dulal Pal, Hiranmoy Mondal: MHD non-Darcian mixed convection heat and mass transfer over a non-linearstretching sheet with Soret–Dufour effects and chemical reaction, International Communications in Heat and Mass Transfer 38, 463–467( 2011).
18. El-Aziz, M. A: Thermal-diffusion and diffusion-thermo effects on combined heat and mass transfer by hydromagnetic three-dimensional free convection over a permeable stretching surface with radiation, Phys. Lett. A, 372(3), 263–272 (2008).

18a El-Aziz, M. A: Flow and heat transfer over an unsteady stretching surface with Hall effects,Mechanica,V.45, pp.97-109(2010).

19. Elbashbeshy EMA, and Bazid MAA, Heat transfer over an unsteady stretching surface, Heat Mass Transfer,41, 1–4(2004).
20. Ferdows, M., Kaino, K., and Crepeau, J. C: MHD free convection and mass transfer flow in a porous media with simultaneous rotating fluid, Int. J. Dyn. Fluids, 4 (1), 69–82 (2008).

20a Grubka,L.J and Bobba,K.M: Heat transfer characteristics of a continuous stretching surface with variable temperature, ASME, J. Heat Transfer,V.107, pp.248(1985).

21. Hirshfelder, J. O., Curtis, C. F., and Bird, R. B: Molecular Theory of Gases and Liquids, 1249, John Wiley, New York. (1954).
22. Jaluria, Y: Natural Convection Heat and Mass Transfer, 326, Pergamon Press, Oxford. (1980).
23. Ishak A, Nazar R, and Pop I, Heat transfer over an unsteady stretching permeable surface with prescribed wall temperature, Nonlinear Anal: Real World Appl, 10, 2909–13(2009).
24. Ishak A, Unsteady MHD flow and heat transfer over a stretching plate, J. Applied Sci, 10(18), 2127-2131(2010).

 

25. Kafoussias, N. G., and Williams, E. W: Thermal-diffusion and diffusion-thermo effects on mixed free-forced convective and mass transfer boundary layer flow with temperature dependent viscosity, Int. J. Eng., 33, 1369–1384 (1995).
26. Kamenetskii, D. A. F: Diffusion and Heat Transfer in Chemical Kinetics, Plenum Press, New York (1969).
27. Makinde, O. D: Free convection flow with thermal radiation and mass transfer past a moving vertical porous plate,Int. Commun. Heat Mass Transfer, 32, 1411–1419 (2005).
28. Makinde, O. D., and Ogulu, A: (2008). The effect of thermal radiation on the heat and mass transfer flow of a variable viscosity fluid past a vertical porous plate permeated by a transverse magnetic field, Chem. Eng. Commun.,195(12), 1575–1584 (2008).
29. Makinde,O.D and Olanrewaju, P.O: Unsyteady mixed convection with soret and Dufour effects past aq porous plate moving through a binary mixture of chemically reacting fluid., Chem.Eng.Comm.V.198, pp.920-938 (2011).
30. Ogulu, A., and Makinde, O. D: Unsteady hydromagnetic free convection flow of a dissipative and radiating fluid past a vertical plate with constant heat flux, Chem. Eng. Commun.,196 (4), 454–462 (2009).
31. Postelnicu, A.: (2007). Influence of chemical reaction on heat and mass transfer by natural convection from vertical surfaces in porous media considering Soret and Dufour effects, Heat Mass Transfer, 43, 595–602 (2007).
32. Rana, M.A, Siddiqui, A.M and Ahmed, N: Hall effect on Hartmann flow and heat transfer of a burger's fluid. Phys. Letters A 372, pp. 562-568(2008).
33. Salem,A.M,Abd El-Aziz,M: Effect of Hall currents and chemical reaction on hydromagtnetic flow of a stretching vertical surface with internal heat generation/ absorption, Applied Mathematical Modelling, V.32,pp.1236-1254(2008)
34. Schlichting, H: (1979). Boundary Layer Theory, 6th ed., 817, McGraw-Hill, New York (1979)..
35. Seddeek, M. A: Thermal diffusion and diffusion thermo effects on mixed free forced convective flow and mass transfer over an accelerating surface with a heat source in the presence of suction and blowing in the case of variable viscosity, Acta Mech. 172(1–2), 83–94. (2004).
36. Sarojamma,G,Mahaoobjan,s and Sreelakshmi,K: Effect of Hall current on the flow induced by a stretching surface., Int. Jour. Scientific and Innovative Mathematical research,V.3(3),pp.1139-1148(2015)
37. Sarojamma, G, Syed Mahaboobjan and V. Nagendramma: Influence of hall currents on cross diffusive convection in a MHD boundary layer flow on stretching sheet in porous medium with heat generation. IJMA, 6(3), pp: 227-248 (2015).
38. Tsai, R., and Huang, J. S: (2009). Heat and mass transfer for Soret and Dufour's effects on Hiemenz flow through porous medium onto a stretching surface, Int. J. Heat Mass Transfer, 52, 2399–2406 (2009).
39. Tsai R, Huang K. H, and Huang J. S, Flow and heat transfer over an unsteady stretching surface with non-uniform heat source, Int. Commun. Heat Mass Transfer, 35, 1340-1343(2008).
40. Wang CY: Liquid film on an unsteady stretching surface, Q Appl Math, 48, 601–610(1990).
41. Watanabe T and Pop I: Hall effects on magnetohydrodynamic boundary layer flow over a continuous moving flat plate. Acta Mech. 108, pp. 35-47, (1995)

**Source of support: Nil, Conflict of interest: None Declared.**